A New Wavelet-Based ECG Delineator for the Evaluation of the Ventricular Innervation

MATTEO CESARI[1], (Member, IEEE), JESPER MEHLSEN[2], ANNE-BIRGITTE MEHLSEN[3], AND HELGE BJARUP DISSING SORENSEN[1], (Member, IEEE)

[1]Department of Electrical Engineering, Technical University of Denmark, 2800 Kongens Lyngby, Denmark
[2]Coordinating Research Centre, Bispebjerg and Frederiksberg Hospitals, 2000 Frederiksberg, Denmark
[3]Department of Clinical Physiology, Nuclear Medicine and PET, Rigshospitalet, 2100 Copenhagen, Denmark
CORRESPONDING AUTHOR: M. CESARI (matteocesari91@gmail.com)

ABSTRACT T-wave amplitude (TWA) has been proposed as a marker of the innervation of the myocardium. Until now, TWA has been calculated manually or with poor algorithms, thus making its use not efficient in a clinical environment. We introduce a new wavelet-based algorithm for the delineation QRS complexes and T-waves, and the automatic calculation of TWA. When validated in the MIT/BIH Arrhythmia database, the QRS detector achieved sensitivity and positive predictive value of 99.84% and 99.87%, respectively. The algorithm was validated also on the QT database and it achieved sensitivity of 99.50% for T-peak detection. In addition, the algorithm achieved delineation accuracy that is similar to the differences in delineation between expert cardiologists. We applied the algorithm for the evaluation of the influence in TWA of anticholinergic and antiadrenergic drugs (i.e., atropine and metoprolol) for healthy subjects. We found that the TWA decreased significantly with atropine and that metoprolol caused a significant increase in TWA, thus confirming the clinical hypothesis that the TWA is a marker of the innervation of the myocardium. The results of this paper show that the proposed algorithm can be used as a useful and efficient tool in clinical practice for the automatic calculation of TWA and its interpretation as a non-invasive marker of the autonomic ventricular innervation.

INDEX TERMS Atropine, ECG wave delineation, metoprolol, wavelets, T-wave amplitude.

I. INTRODUCTION

The generation of electrical impulses and the conduction of electrical signals through the heart is influenced and regulated by the Autonomic Nervous System (ANS), which is divided into two branches: the Sympathetic Nervous System (SNS) and the Parasympathetic Nervous System (PNS) [1].

The PNS innervates primarily the sinoatrial (SA) and atrioventricular (AV) nodes through the vagus nerve and its efferent fibers release the neurotransmitter acethylcholine that binds to muscarinic receptors in the heart. In resting conditions, the PNS has the greatest impact on the autonomic regulation of the heart and its main effects are the decreases of heart rate, force of atrial contraction and conduction velocity in the SA and AV nodes. On the other hand, the SNS innervates the SA and AV nodes, and the ventricles and its fibers release norepinephrine to beta-adrenergic receptors. Its effects are opposite to the ones of the PNS, therefore it has the greatest impact in stressing situations [1].

The ANS plays an important role in the regulation of physiological and pathophysiological conditions such as myocardial infarction, arrhythmias, and autonomic dysfunctions. In the clinical world, there are currently several methods for assessing the status of the ANS such as cardiovascular reflex tests, biochemical tests, and techniques that give direct access to the receptors at a cellular level. These methods are usually invasive and expensive [2].

During the last three decades, a number of techniques based on the electrocardiogram (ECG) have been developed for monitoring the cardiac ANS. The most known is the analysis of the Heart Rate Variability (HRV). Briefly, the HRV consist on a series of RR intervals originating in the SA and it is thought to reflect the adaptability of heart rate to various stimuli [2], [3]. HRV analysis can be made in the time or frequency domain and by non-linear analysis. Several publications have proposed the power spectral analysis of the HRV as a useful tool to evaluate the sympatho-vagal balance

at the sinoatrial level for patients in sinus rhythm with only few ectopic beats [2]–[5].

Because of the origin of HRV, it can primarily be used to evaluate the innervation of the SA node and it does not provide any information on the ventricular innervation. In the clinical world, a non-invasive method for this purpose is highly desirable for applications such as monitoring the re-innervation after cardiac transplantation, and studying the origin of arrhythmias and several autonomic dysfunctions.

The T-wave in the ECG is most likely generated by the differences in the repolarization time among the different layers of the ventricular myocardium and it has been proved that the ANS is able of regulating the action potential duration of the myocytes and – most likely – also the dispersion between myocardial layers [6], [7]. For these reasons, it is believed that the analysis of the T-wave could be used as a non-invasive method to monitor the ventricular innervation.

Several studies have shown that T-wave amplitude (TWA) may be a marker of the autonomic innervation of the myocardium. In particular, it has been shown that blocking the PNS with anticholinergic drugs (i.e. atropine) and activation of the SNS with head-up tilt cause a significant decrease of TWA, while blocking the SNS with beta-adrenoceptor antagonists provokes its significant increase [8]–[11]. In order to calculate TWA, these studies rely on manual annotations [8], [9], or on software performing ECG waveform averaging that still require human interaction [10], [11]. Thus, the absence of completely automatic methods to evaluate the TWA make the research in this field time-consuming and not directly applicable in the clinical world.

Nevertheless, several completely automatic methods for the delineation of ECG waveforms have already been proposed in literature and they use the phasor transform [12], the properties of the wavelet transform [13]–[16], hybrid hidden Markov models combined with the wavelet transform [17], [18], and mathematical models [19] among others. A comparison of the performances of these different approaches revealed that the algorithms based on the Wavelet Transform (WT) achieved good performances in the delineation of the ECG fiducial points. Moreover, the WT is attractive as a mathematical tool because of two main properties. First, when the WT is applied, the ECG can be described at different scales of temporal and frequency resolution, thus high frequency waves (such as the QRS complex) can be distinguished from low frequency waves (such as P and T waves). Second, the WT can be easily implemented with a cascade of Finite-Impulse Response (FIR) filters [16].

In this context, the present paper has two main aims: (*i*) to present a new wavelet-based algorithm for the delineation of ECG fiducial points that takes inspiration from some state-of-the-art methods and further elaborates them and (*ii*) to apply the new algorithm to data recorded in healthy subjects that were treated with anti-adrenergic and anti-cholinergic drugs in order to automatically evaluate the changes in TWA related to the changes in activity of the cardiac ANS. In this way, this paper proposes for the first time a reliable and automatic method for the evaluation of the innervation of the ventricles.

The paper is organized as follows: in Section II the data used for the work, the mathematical theory behind the WT, the new algorithm and the methods for the statistical analysis of the results are explained; in Section III the results of the validation of the algorithm and the ones obtained with the application of the algorithm to the experimental data are shown; in Section IV the results are discussed and finally Section V concludes the work.

A preliminary version of this study has been presented in [20].

II. METHODS
A. DATA
In this study, three different ECG databases were used. In particular, an experimental database was used for algorithm development, validation and for evaluating the changes of TWA in relation to the ANS, while the two standard QT and MIT/BIH Arrhythmia databases were used in order to validate the proposed algorithm. A brief description of the databases is now provided.

1) EXPERIMENTAL DATABASE
Eight healthy, male volunteers (25.3 ± 2.7 years) participated in this study. At the time of the study, they did not have a history or clinical evidence of diabetes mellitus, heart disease or bronchial asthma and they were non-medicated. They were randomly studied in two days in a cross-over study. In one day, they received constant infusion of isotonic saline (total volume 50 mL) with the subsequent addition of atropine and series of head-up tilt as described below. The other day they were given constant infusion of the beta-1-adrenoceptor-antagonist metoprolol. Metoprolol was given as a priming dose of 5 mg and then followed by constant infusion of 0.025 mg min^{-1} kg^{-1}. In both days, thirty minutes after starting the continuous infusion, the subjects were tilted head-up at an angle of $60°$ and after approximately 10 minutes tilted down. Four boluses of atropine (0.0025 mg kg^{-1}) were given with an interval of 20 minutes. After each bolus of atropine, the tilt up and tilt down were repeated. During all the experimental phases and five minutes before the beginning of the continuous infusion (for baseline reference), the ECG was continuously recorded by one precordial lead with the ADInstruments®Bioamp connected through a ADinstruments®Powerlab 8/35. The sampling frequency was set at 1 kHz.

Ethical Review Board approved the study and the subjects signed the informed consent.

2) MIT/BIH ARRHYTHMIA DATABASE
The MIT/BIH Arrhythmia Database (MITDB) [21] contains 48 30-minute length 2-lead Holter recordings with clinical relevant phenomena, where the QRS complexes were manually annotated. The signals were recorded with a sampling frequency of 360 Hz.

3) QT DATABASE

The QT database (QTDB) [22] includes 105 2-lead recordings of 15 minutes duration where at least 30 QRS complexes, T-waves, P-waves and their onsets and offsets were annotated by one cardiologist (*ref1*). For 11 recordings, a second cardiologist (*ref2*) annotated the same beats as *ref1*. The signals were recorded with a sampling frequency of 250 Hz.

B. THE WAVELET TRANSFORM

The WT is a decomposition of a signal $x(t)$ into a set of basis functions, that are obtained by dilatation (a) and translation (b) of a mother wavelet $\psi(t)$. The WT of $x(t)$ is defined as [14]:

$$W_a[x(t)] = \frac{1}{\sqrt{a}} \int_{-\infty}^{+\infty} x(t) \cdot \psi\left(\frac{t-b}{a}\right) dt, \quad a > 0 \quad (1)$$

The WT has high temporal resolution at high frequency and low temporal resolution at low frequencies, thus achieving the time-frequency decomposition of the signal $x(t)$. For the choice of $\psi(t)$, it is recommended to use a mother function that resembles the most the signal to be analysed [23].

It is also important to mention another property that will be used later for T-peak detection. Consider now a *smoothing function* $\theta(t)$, the signal

$$Y_a[x(t)] = \int_{-\infty}^{+\infty} x(t) \cdot \theta\left(\frac{t-b}{a}\right) dt \quad (2)$$

and its derivative calculated with respect to b :

$$\frac{\partial Y_a[x(t)]}{\partial b} = -\frac{1}{a} \int_{-\infty}^{+\infty} x(t) \cdot \theta'\left(\frac{t-b}{a}\right) dt \quad (3)$$

Now, if $\psi(t) = \theta'(t)$, (i.e. the mother wavelet is the derivative of a smoothing function) it follows that :

$$W_a[x(t)] \propto \frac{\partial Y_a[x(t)]}{\partial b} \quad (4)$$

Therefore, the WT at scale a is proportional to the quasi-convolution derivative of the signal $x(t)$ and $\theta(t)$ [16]. From this property, it follows that zero-crossings of the WT correspond approximately to local extrema of the smoothed signal $x(t)$ and that local extrema of the WT are related to areas with maximum slope in the smoothed signal.

In case of discrete signals, the parameters a and b are discretized by applying a dyadic scale: $a = 2^k$ and $b = 2^k l$. The basis function of the *dyadic wavelet transform* therefore becomes:

$$\psi_{k,l}(t) = 2^{-k/2} \psi(2^{-k}t - l); \quad k, l \in Z^+ \quad (5)$$

Once the dyadic scale is applied, also the time has to be discretized for discrete signals. Mallat [24] proposed the traditional implementation of the Discrete Wavelet Transform (DWT) and it corresponds to a filter bank. Each mother wavelet is associated with a low-pass FIR filter $H(f)$ and a high-pass FIR filter $G(f)$ that are properly combined to obtain the levels of decomposition of the signal. In this implementation, the signal is downsampled by a factor 2 at each stage; therefore its length is halved. This is shown in Fig. 1(a).
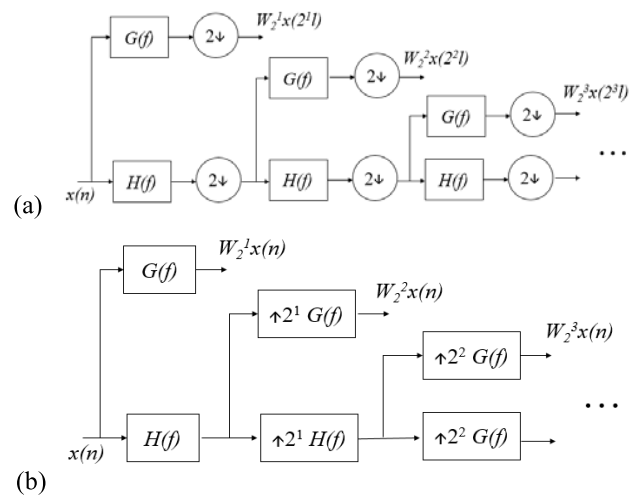

FIGURE 1. Implementation of the DWT with Mallat algorithm (a) and with the SWT (b). Redrawn from [14].

Because of the downsampling, the original resolution of the signal is lost and this could make the identification of characteristic points more difficult and less precise. For this reason, the Stationary Wavelet Transform (SWT) has been proposed as an alternative implementation of the WT in discrete time. In this case, the filters are upsampled by a factor 2 at each stage (Fig 1(b)). Therefore, the WT at each scale has the same length of the original signal, thus keeping its original resolution [25]. The equivalent frequency response of the filters at scale k is:

$$Q_k(f) = \begin{cases} G(f) & k = 1 \\ G(2^{k-1}f) \prod_{l=0}^{k-2} H(2^l f) & k \geq 2 \end{cases} \quad (6)$$

C. ALGORITHM DESCRIPTION

The objective of the algorithm is to calculate automatically TWA for each beat of the ECG signal. In order to do that, the algorithm delineates QRS complexes, T-wave peaks (upwards, inverted and biphasic), T-wave ends and estimates the baseline level beat by beat. All these steps are now explained in details. We implemented the algorithm in Matlab®2015b. The algorithm here described was designed for the experimental database, therefore the following steps apply to a sampling frequency of 1 kHz. With slight modifications the algorithm can be applied to other sampling frequencies, as it will be outlined for the MIT/BIH and QT databases.

1) ECG PREPROCESSING

The software system for the acquisition of the data applies a bandpass filter with cutoff frequencies at 1 and 40 Hz. In this way, the high frequency noise and the baseline wander are removed from the signal. An example of recorded and filtered ECG signal is shown in Fig. 2(a).
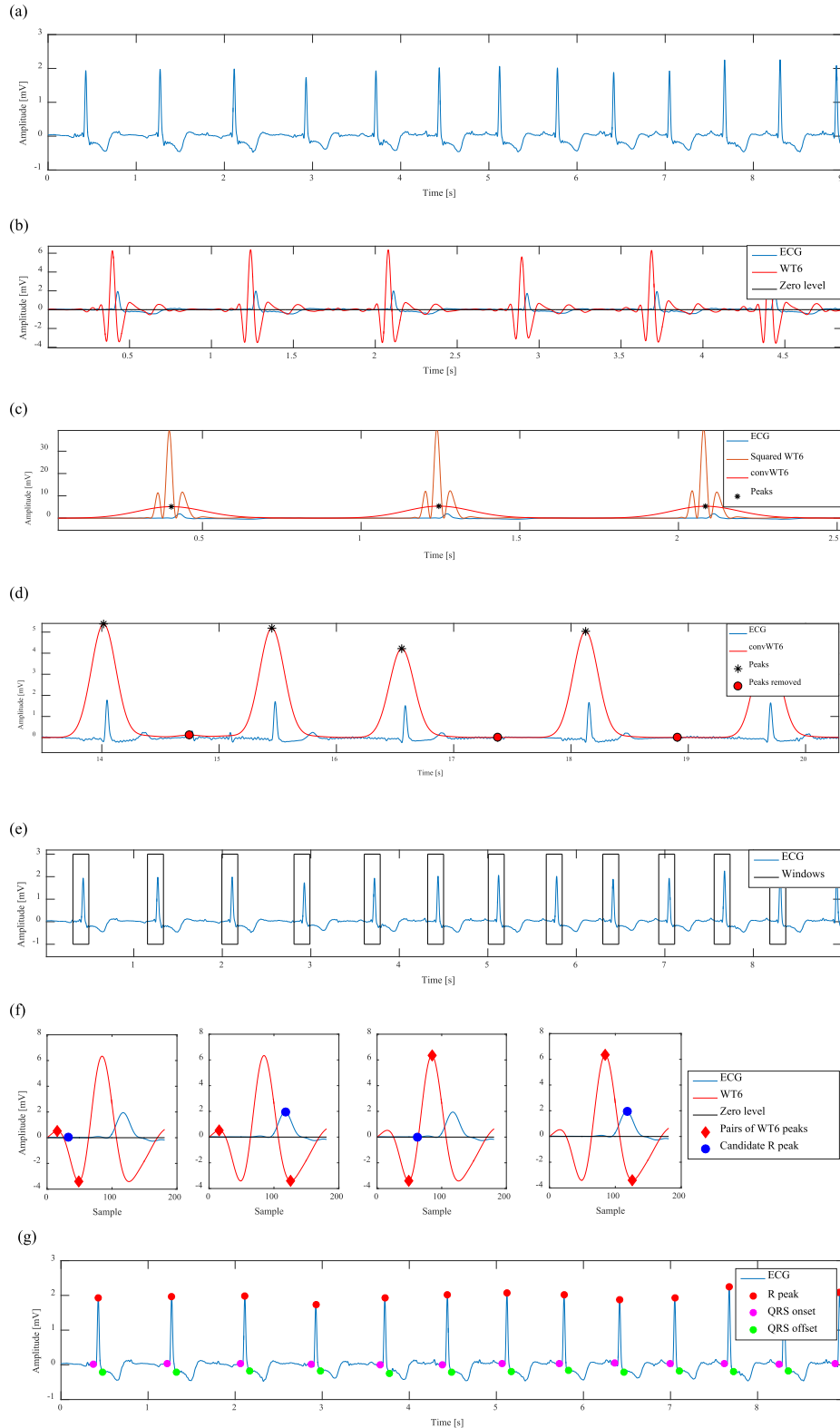
FIGURE 2. Example of detection of QRS complexes in an ECG signal. (a) ECG signal used for the analysis.
(b) ECG signal and correspondent WT at the sixth scale calculated with the Daubechies 3 mother wavelet.
(c) ECG signal, WT squared and the signal obtained with the convolution of the WT with a Gaussian kernel
with standard deviation of 100 ms and respective peaks. (d) Example of removed noisy peaks.
(e) Windows where the QRS complexes are expected to be located. (f) Example of detection of R-peak.
In each window pairs of positive and negative peaks are found and for each pair a candidate R-peak is
obtained. The one with the most significant peaks in WT6 and candidate R-peak is chosen as R-peak.
(g) Detected R peaks, QRS onsets and QRS offsets.

2) QRS DETECTION AND DELINEATION

For QRS detection and delineation, we developed an algorithm that takes inspiration from the work of Merah *et al.* [25], but several differences between the two methods were implemented and they will be outlined below.

First, we decided to apply the Daubechies *db3* mother wavelet with the SWT algorithm. This mother wavelet is not related to any smoothing function, therefore the property in Eq. (4) does not apply. In order to enhance the QRS complexes and suppress other ECG waves, the 6th scale of the SWT (*WT6*) was chosen. In fact, due to the SWT implementation, this scale enhances the frequency band which characterizes QRS complexes and filters out P and T-waves [26]. An example of WT6 signal is shown in Fig. 2(b).

The next step is the localization of the areas where the QRS complexes are expected to be positioned. In order to do that, the *WT6* signal is squared and the resulting signal is convolved with a Gaussian kernel with standard deviation of 100 ms (Fig 2(c)). The resulting signal is now referred as *convWT6*. This step is not performed in [25].

The peaks in *convWT6* are then found by searching local maxima in the signal (Fig. 2(c)) and grouped in sets of 10 peaks. For each group, the root mean square (RMS) of the peak values is calculated and the ones having amplitude lower than $0.1 \times$ RMS are removed since they are considered noisy peaks (Fig. 2(d)). For each of the remaining peaks in *convWT6*, a window of length 180 ms (*W*) centered in the peak is obtained and this is considered the window where a QRS complex is expected to be located (Fig. 2(e)).

Once the windows *W* are selected, the algorithm proceeds with the identification of the R peaks. In each window, the positive (*P*) and negative (*N*) peaks of the *WT6* are found. All the *M* combinations of one positive and one negative peaks are analyzed. For each combination $i = 1, \ldots, M$ of peaks, if the positive peak P_i precedes the negative peak N_i, the maximum of the ECG between P_i and N_i is searched and it is labeled as the candidate R peak (whose amplitude is c_{Ri}). In the case of negative peak preceding a positive one, the minimum is searched. An example of pairs of peaks and selection of candidate R-peaks in a window is shown in Fig. 2(f). For each combination *i,* the index $s_i = |c_{Ri}| + |WT6(P_i)| + |WT6(N_i)|$ is calculated and the candidate R peak having the highest value of s is selected as R-peak. In the case of the example shown in Fig. 2(f), the last combination is the one that identifies the R-peak. The index s is a compact index that contains the information of both the WT and the ECG signal and has never been proposed in literature.

The QRS onset and QRS offset are then identified by searching the first zero-crossing of the WT before and after the identified R peak, as proposed in [25].

A post-processing phase is then applied to remove the errors in R-peak detection. One of the following two criteria should be met for removing wrongly identified peaks:
- If two or more peaks are identified in a window of 250 ms, the one with the highest amplitude is kept as R-peak and the others removed;
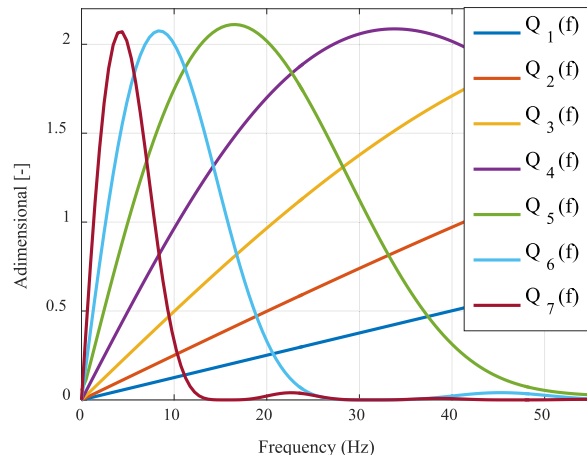

FIGURE 3. Frequency response of the SWT up to scale with the mother wavelet proposed in [14] at a sampling frequency of 1 kHz.

- From the detected R peaks, the RR intervals are calculated. For each RR interval, the set of the previous and following 10 RR intervals is considered. The median (*m*) of the set is calculated and if the selected RR interval has duration lower than $0.4 \times m$, only the R peak with the highest absolute amplitude is kept and the other removed.

In Fig. 2(g) an example of the identified R peaks, QRS onsets and QRS offsets is shown.

3) FILTERING

Since the frequency content of the T-wave is up to 10 Hz [27], we decided to filter the signal with a Butterworth zero-phase low-pass filter of order 8 and cut-off frequency of 20 Hz. This filter removes the high frequency noise in the T-waves and does not alter their frequency content.

4) T-PEAK IDENTIFICATION

For the identification of the T-peaks, the mother wavelet proposed in [13]–[16] was chosen. The Fourier Transform of this mother wavelet is:

$$\Psi(f) = j2\pi f \left(\frac{\sin\left(\frac{2\pi f}{4}\right)}{\left(\frac{2\pi f}{4}\right)} \right)^4 \qquad (7)$$

It can be seen that the mother wavelet corresponds to the derivative of the convolution of four rectangular pulses [14]. This means that the mother wavelet is the derivative of a smoothing function, therefore the property of Eq. (4) is applicable. The low-pass and high-pass filter corresponding to this mother wavelet are respectively:

$$H(f) = e^{\frac{j2\pi f}{2}} \left(\cos \frac{2\pi f}{2} \right)^3 \qquad G(f) = 4je^{\frac{j2\pi f}{2}} \left(\sin \frac{2\pi f}{2} \right) \quad (8)$$

The frequency response of the filter $Q_k(f)$ can be seen in Fig. 3 for a sampling frequency of 1 kHz. It was chosen to consider the 6th scale of the WT (labelled as *WT6*) for the
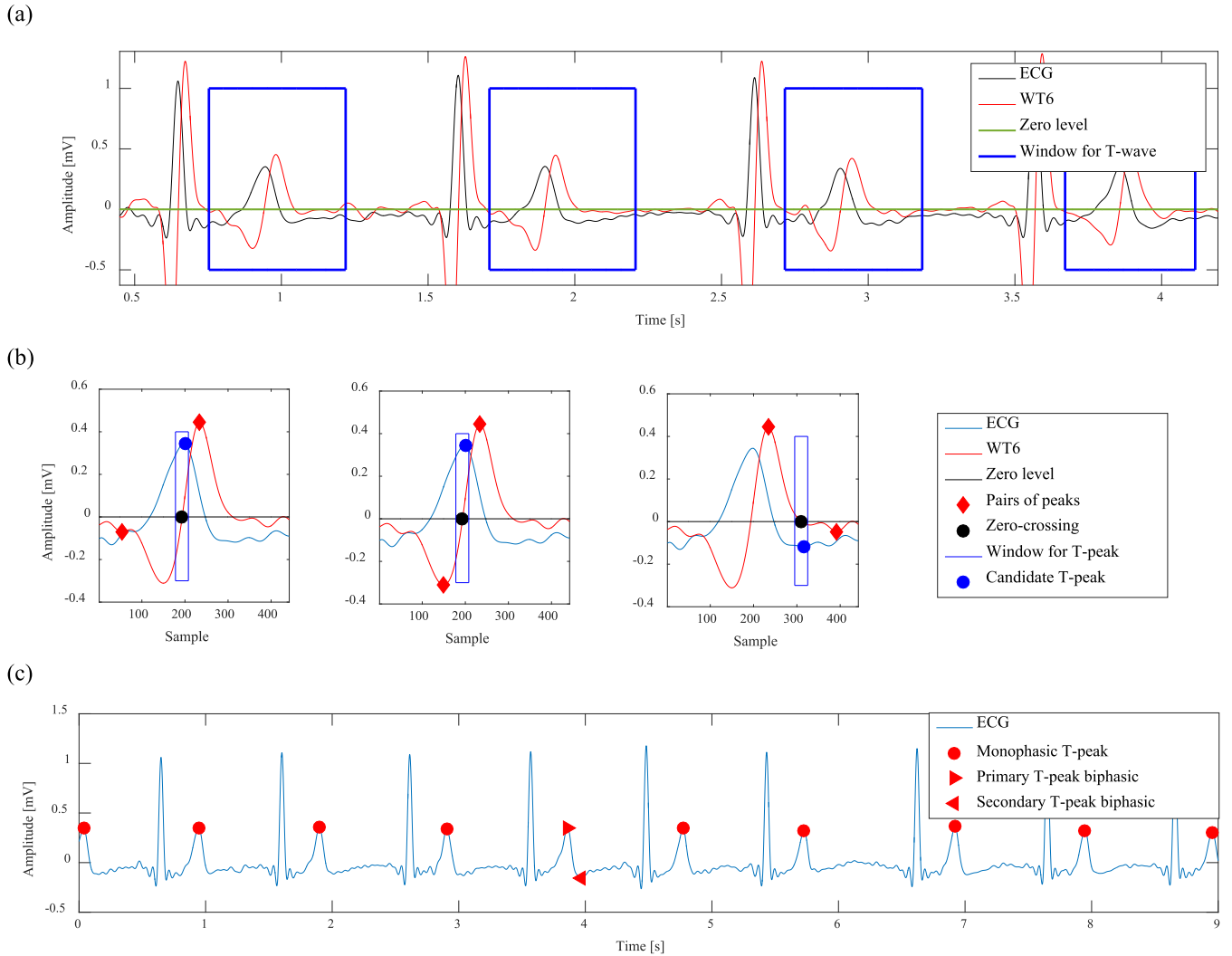
(a)

(b)

(c)

FIGURE 4. Delineation of the T-peaks. (a) Selection of the window where the T-peak is expected. The ECG, WT and zero-level are represented. (b) Example of detection of the primary T-peak in a window. The pairs of peaks of the WT are considered and the zero-crossing $\hat{z}$ between them is used to identify the candidate T-peak in a 30 ms window. In this window, the second candidate T-peak is the one selected as primary T-peak. (c) Detection of the T-peaks. Note that one T-wave is wrongly considered biphasic. The mistake will be corrected with the delineation of the T-end points.

T-peak detection because its frequency band fits the frequency content of the T-wave and because it was giving defined peaks in correspondence of T-waves.

In order to detect the T-peaks, the following steps are applied:

1) For each beat *i* a searching window for the T-wave is defined as : $W(i) = [QRS_{off}(i) + 50\ ms, R(i) + 0.6 \times (R(i+1) - R(i))]$, where QRS_{off} is the QRS offset and R the R-peak. In Fig. 4(a) an example of selected windows is shown.
2) For each window i, the positive (P) and negative (N) peaks of the *WT6* are found.
3) The mean of the positive peaks (m_P) and negative peaks (m_N) are calculated. The positive peaks having amplitude lower than $0.4 \times m_P$ and the negative ones with amplitude higher than $0.3 \times m_N$ are removed because of their low amplitude.

4) The M zero crossings $z_1, \ldots, z_M$ of the *WT6* are located in each window.
5) The *pairs* of positive and negative peaks that are closer than 200 ms are found. This is done because a T-wave is defined by a positive and negative slopes and because the duration of the T-wave is lower than 200 ms [28].
6) Each pair of peaks is then analyzed. If the negative peak N precedes the positive peak P, a positive T-wave is expected. All the zero crossings $z_i\ i = 1, \ldots, Z$ between N and P are considered and the zero-crossing in correspondence of the highest ECG value is labelled as $\hat{z}$. The maximum value of the ECG in a window of 30 ms around $\hat{z}$ is chosen as the candidate T-peak (whose amplitude is c_{Ti}). In case of negative peak following a positive one, the lowest ECG value is searched. An example of pairs of *WT6* peaks, zero-crossing $\hat{z}$ between them, searching window for the T-peak and candidate T-peak is shown in Fig. 4(b).

7) For each pair i, the index $S_i = 1.5|WT6(N_i)| + 1.5|WT6(P_i)| + |c_{Ti}|$ is calculated and the candidate T-peak with the highest value of S_i is defined the primary T-peak (T_P) and the respective index as S_P. In the case of the example proposed in Fig. 4(b), the second candidate T-peak is the one with the highest S value. This index has never been proposed in literature before and it summarizes the main properties of the T-wave. In fact, the T-wave is characterized by significant slopes (defined by the peaks in the $WT6$) and by significant amplitude in the ECG signal (defined by the candidate T-peak).

8) A check for the possible presence of biphasic T-waves is then performed. If T_P is positive, the secondary lobe of a biphasic T-wave is negative and it may occur either before or after it. For this reason, the pairs of $WT6$ peaks having in common one peak of the ones used for identifying T_P are analyzed. For each of these pairs, the candidate secondary T-peak is found and the index S calculated in the same way described before. The candidate secondary T-peak having the highest index value is chosen and its index labelled as S_S. If $S_S > 0.6S_P$, the T-wave is considered biphasic and it is characterized by the primary and secondary T-peaks, otherwise the primary T-peak constitutes the T-peak of a monophasic T-wave. An example of T-peaks detection is shown in Fig. 4(c). It can be noticed that a biphasic T-wave is wrongly detected around the 4th second in Fig. 4(c). The mistake will be corrected with the delineation of T-end points.

5) T-END DELINEATION

The algorithm then delineates the T-end points. In order to do that, the approaches proposed by Ghaffari *et al.* [15] and Zhang *et al.* [29] are combined.

Zhang *et al.* [29] proposed a robust and efficient method for T-end delineation, that is here reported. Inside each ith RR interval, two points k_a and k_b are defined with the following rules:

$$k_a = \begin{cases} R_i + \lfloor 0.15RR_i \rfloor + 37(fs/250) & RR_i < 220(fs/250) \\ R_i + 70(fs/250) & otherwise \end{cases} \quad (9)$$

$$k_b = \begin{cases} R_i + \lceil 0.7RR_i \rceil - 9(fs/250) & RR_i < 220(fs/250) \\ R_i + \lceil 0.2RR_i \rceil + 101(fs/250) & otherwise \end{cases} \quad (10)$$

where fs is the sampling frequency.

For each sample $k = k_a, \ldots, k_b$ the following values are computed:

$$\bar{s}_k = \frac{1}{2p+1} \sum_{j=k-p}^{k+p} s_j \quad (11)$$

$$A_k = \sum_{j=k-w+1}^{k} (s_j - \bar{s}_k) \quad (12)$$

where $w = 128 \cdot (fs/1000)$ and $p = 16 \cdot (fs/1000)$, and s_j is the jth sample of the ECG signal. The value A_k represents the area of the signal inside the sliding window w that is moved in the selected signal. After the calculation of A_k for each value k, the following values are found:

$$k' = \underset{ka \leq k \leq kb}{\arg\max} A_k \quad k'' = \underset{ka \leq k \leq kb}{\arg\min} A_k \quad (13)$$

Now, if

$$\frac{1}{\lambda} \leq \frac{|A_{k'}|}{|A_{k''}|} \leq \lambda \quad (14)$$

where we arbitrarily set the value $\lambda = 2$, the T-end with this first method is located at

$$T_{end1} = \max(k', k'') \quad (15)$$

Otherwise, it is located at

$$T_{end1} = \underset{k \in \{k', k''\}}{\arg\max} |A_k| \quad (16)$$

We decided to add another step to this algorithm. In fact, it was seen that in case of tall U and P waves, the algorithm detects the T-end at the peak of the U or P waves. To correct this, the T_{end1} with absolute amplitude greater than the half of the absolute amplitude of the respective T-peak were removed. In case of biphasic T-waves, the T-peak with the highest absolute amplitude was considered for that purpose. An example of location of T_{end1} points is shown in Fig 5(a).

Ghaffari *et al.* [15] proposed the Area Curve Length (ACL) measure for the delineation of fiducial points in the ECG. The $WT6$ signal proposed in Section II.A.4 is used for this purpose. A window of length $L = 40$ ms is considered and the vector $Y_k = WT6[k : k + L]$ is used for calculating:

$$A(k) = \sum_{k=t_{0k}}^{t_{fk}} |y_k| \quad c(k) = \sum_{k=t_{0k}}^{t_{fk}} \sqrt{1 + (y_k - y_{k-1})^2} \quad (17)$$

where t_{0k} and t_{fk} are the initial and final points of Y_k and y_k its samples. The ACL measure is then calculated as $ACL(k) = A(k) \times c(k)$. An example of ECG and the respective ACL value is shown in Fig. 5(b). Minimum values of ACL are obtained in correspondence to areas with minimum amplitude and slope. For this reason, the first local minimum after T-peak is considered the location of the T-end point with this second method (T_{end2}). In case of biphasic T-waves, two points ($T_{end2,1}$ and $T_{end2,2}$) are obtained (Fig 5(c)).

At this point, in order to find the T-end point, the two methods are combined with the following rules:

- In case of monophasic T-wave, if T_{end1} and T_{end2} are within a window of 50 ms, their average position is considered as the T-end. Otherwise, the one with the lowest ACL value is considered the T-end.
- In case of biphasic T-wave, if one of $T_{end2,1}$ or $T_{end2,2}$ is within 50 ms from T_{end1}, their average position is considered the T-end point, otherwise the one with the lowest ACL value is the T-end.
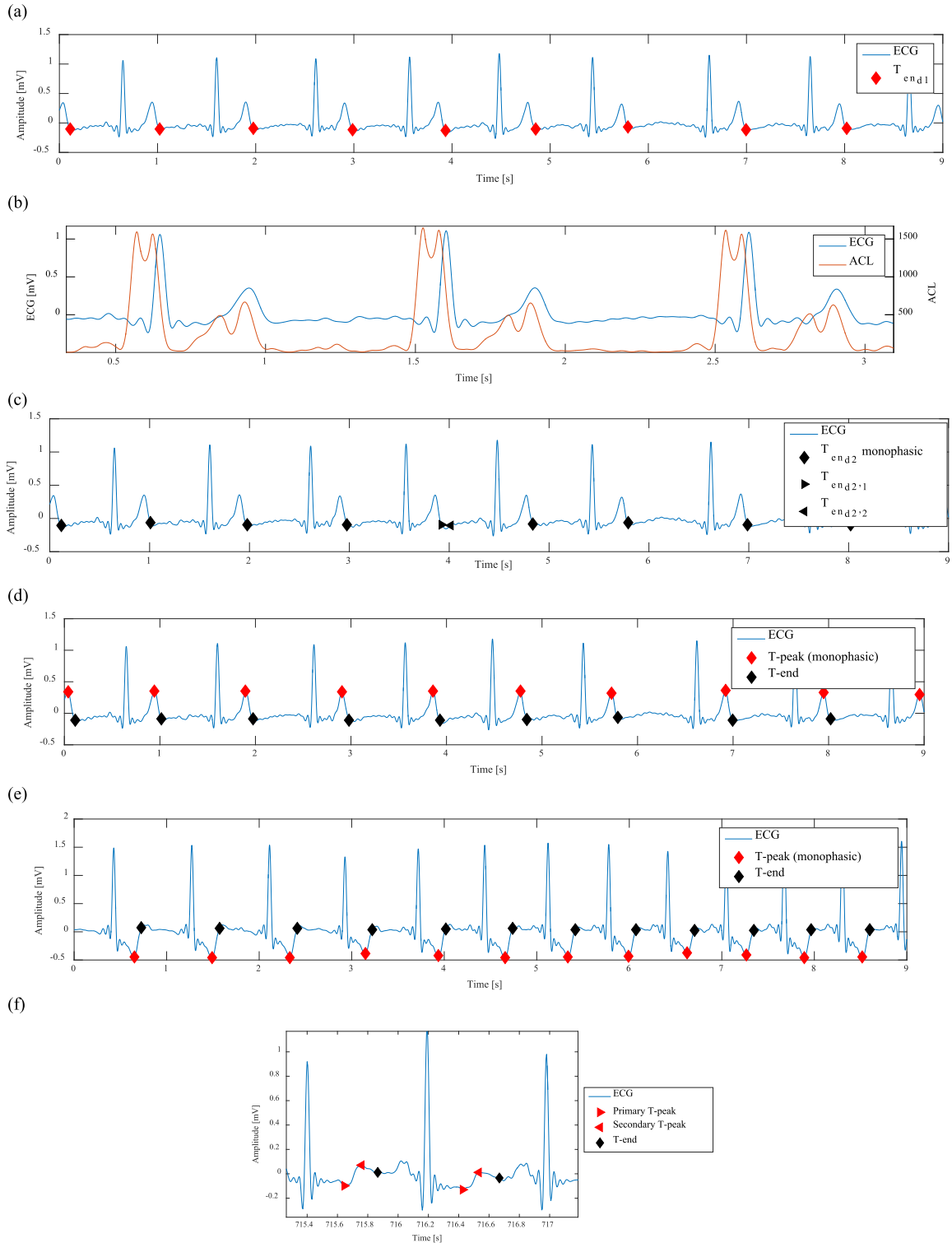
FIGURE 5. Delineation of the T-end points. (a) Identification of the T-end points with the method proposed by Zhang *et al.* [29]; (b) ECG and ACL measure proposed by Ghaffari *et al.* [15]. (c) Identification of the T-end points with the ACL method. (d) Final identification of the T-peaks and T-end points in case of upwards T-waves; Note that the mistake in the identification of T-peak presented in Fig. 4(c) is now corrected. (e) Final identification of T-peaks and T-end points in case of inverted T-waves; (f) identification of biphasic T-waves and their end points.

- In case of absence of T_{end1}, the T_{end2} or the point with the lowest ACL value between $T_{end2,1}$ and $T_{end2,2}$ is the T-end.

In case of a previously detected biphasic T-wave, an additional check is performed. In particular, if the so identified T-end point is located before the secondary T-peak, the

biphasic T-wave is re-annotated as monophasic and only the primary peak considered. Instead, if the detected T-end is located after the secondary T-peak, nothing is changed on the detected primary and secondary T-peaks and the T-wave is still considered biphasic.

In Fig. 5(d) the same signal of Fig. 4(c) is shown and it is possible to observe that the proposed method is able to correct the mistake in T-peak detection. In particular, the wrongly detected biphasic T-wave is re-annotated as monophasic. In general, this method is able of detecting correctly normal, inverted T-waves and biphasic T-waves and their end points as shown in Fig. 5(d), 5(f) and 5(g) respectively.

6) BASELINE ESTIMATION

The next step of the algorithm is the estimation of the baseline level in the TP segment. In order to do that, first for each beat i the window $B_i = [T_{end}(i) + 50\ ms, QRS_{on}(i+1) - 100\ ms]$ is selected. Three methods are combined for the baseline estimation:

1) *ACL Method:* the index with the minimum ACL value is found in B_i. The baseline is estimated as the median value of the ECG signal in a 20 ms window around the selected point.
2) *Slope Method 1:* for each sample k in B_i the index $r_k = |ECG(k)-ECG(k+25ms)|$ is calculated. The index $\hat{k}$ corresponding to the lowest value of r_k is considered and the baseline is estimated as the mean of the ECG signal in the interval $[\hat{k}, \hat{k} + 25ms]$.
3) *Slope Method 2:* for each sample k in B_i the window $W_k = [ECG(k), ECG(k) + 40ms]$ is considered. The windows is downsampled at 250 Hz (W_k^d), its derivative calculated ($\dot{W}_k^d$) and the parameter $S_k = \sum_i \dot{W}_k^d(i)$ obtained. The median of the window having the lowest value of S is the estimation of the baseline level.

When the three baseline levels are estimated, the two that differ the least are considered. The final baseline estimation is obtained by averaging them.

7) TWA CALCULATION

The TWA is calculated by considering the absolute value of the difference between the T-peak and the baseline level. In case of biphasic T-wave, the peak giving the highest value of TWA is considered. An example of TWA calculation is shown in Fig. 6.

D. VALIDATION OF THE FIDUCIAL POINTS LOCATION

To assess the performances of the developed method for fiducial point delineation, we evaluated the difference between automatic and manual annotations in the MITDB, QTDB and experimental databases described in Section II.A. In particular, we calculated sensitivity $Se = TP/(TP + FN)$, positive predictivity $P^+ = TP/(TP + FP)$ and detection error $Er = (FN + FP)/TB$, where TP denotes the true positives (when an automatic annotation matches a manual
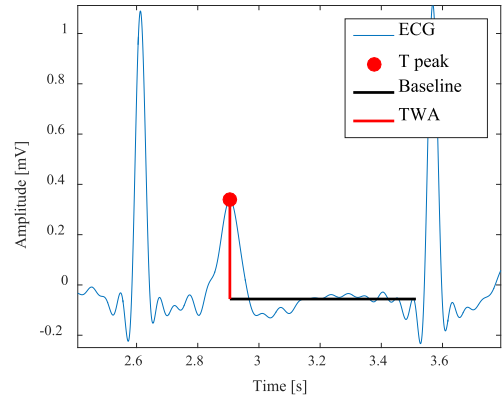

FIGURE 6. Example of calculation of TWA.

annotation), FN the false negatives (when for a manual annotation there is not correspondent automatic annotation), FP the false positives (when for an automatic annotation there is not correspondent manual annotation) and TB the true beats. In order to consider an automatic annotation a TP, it should fall within a certain window w from the manual annotation [14].

We evaluated also the delineation accuracy of the algorithm. In particular, we calculated the time difference (i.e. error) between automatic and manual annotations. We obtained the values of m as the average of the errors and s as the average of the standard deviation of the errors obtained for each record in the evaluated databases. However, the value m does not give an appropriate idea of the precision, because outliers with opposite signs can be averaged out. For this reason, we calculated $|M|$ as the average of the absolute values of the errors across all the records as proposed in [30].

The MITDB and QTDB use a sampling frequency of 360 and 250 Hz respectively. When dealing with different sampling frequency, one option would be to upsample the signals to 1 kHz. In this case, this approach might introduce errors in the positions of the manual annotations, thus leading to wrong results. Another approach would be to resample the filters, but this approach would require a lot of work for different sampling frequencies. Therefore it was chosen to slightly modify the algorithm by choosing the 4th scale of the WT for both QRS and T-wave delineation for those signals in order to detect the fiducial points. Moreover, for the delineation of T-end points in the QT database with the method proposed by Zhang et al. [29] we used the value of $\lambda = 6$ as in the original work.

As outlined before, the signals of the experimental database were filtered by the software in the range 1-40 Hz. The same result was achieved in the international databases by applying the pre-processing procedure proposed by Banarjee *et al.* [31].

E. STATISTICAL ANALYSIS

In the experimental database, the obtained values of TWA were used for analyzing the changes of TWA related to

TABLE 1. QRS detection performance comparison in the MIT/BIH Arrhythmia database. For each work, the window used for defining a true positive is reported (*w*), together with the number of true beats (TB), true positives (TP), false positives (FP), false negatives(FN), sensitivity (Se), positive predictivity (P⁺) and detection error (Er) (N/R: Not Reported).

Method	w[ms]	TB	TP	FP	FN	Se[%]	P+[%]	Er[%]
This work	**150**	**109494**	**109321**	**147**	**173**	**99.84**	**99.87**	**0.29**
Ghaffari et al. [16]	150	109428	109367	89	61	99.94	99.91	0.14
Ghaffari et al. [15]	150	109428	109327	129	101	99.91	99.88	0.21
Benitez et al. [32]	150	N/R	N/R	187	203	99.81	99.83	0.36
Saadi et al. [33]	150	N/R	N/R	N/R	N/R	99.87	99.90	N/R
This work	**100**	**109494**	**109297**	**176**	**197**	**99.82**	**99.84**	**0.34**
Merah et al. [25]	100	109494	109316	126	178	99.84	99.88	0.28
Martinez et al. [14]	N/R	109428	109208	153	220	99.80	99.86	0.34
Pan and Tompkins [34]	N/R	109809	109532	507	277	99.75	99.54	0.71

the ANS. For each experiment, the two minutes of ECG before tilting and the period from the first to the third minute after tilt were used for the analysis of the results. By hypothesizing a heart rate of 60 beats/min, for each of the condition analyzed around 120 repeated measurements from each subject were available.

In order to compare the different treatments by taking into account both the inter-subject and intra-subject variability, we developed the following mixed effect linear model

$$TWA_{ij} = c_{ij} + N(0, \sigma_1)|_j + N(0, \sigma_2)|_j + \varepsilon_{ij} \quad (18)$$

Where c_i is the *i*th condition studied (e.g. first tilt up, supine position after the first dose of atropine, etc.) and the two Gaussian distributions model the inter-subject variability and the intra-subject variability (due to the repeated measurements). The index *j* represents the *j*th repeated measurement for the *i*th condition. Moreover, since the repeated measurements are consecutive in time, we decided to model their correlation with an auto-regressive model of order 1 [38], [39].

III. RESULTS
A. VALIDATION
In the following paragraphs, the results of the validation of fiducial point delineation on MIT/BIH, QT and the experimental database are shown.

1) MIT/BIH ARRHYTHMIA DATABASE
In Table 1, the performances of the algorithm in the MIT/BIH database with window size $w = 150\ ms$ and $w = 100$ ms are shown and compared to the literature.

For the purpose of comparing the algorithm with other works, we applied it to the first lead in each recording. Moreover, we excluded the segments with ventricular flutter in record 207.

2) QT DATABASE
When the recordings of the QT database were annotated, the manual annotations were performed by visualizing both the leads. Because of that and for the fact that the developed

algorithm works only in one lead, we chose for each annotation the lead that was producing less error [12], [14]–[16]. In this way, we calculated *Se* by considering a $w = 150$ ms for the *TP*. For the QTDB, some parts of the recordings between sets of annotated beats were not scored by the cardiologists. In these cases, it is not possible to establish whether the cardiologists considered that no wave was present or they could not perform a proper annotation. For this reason, it is not possible to accurately calculate the positive predictivity under these conditions.

The results and the comparison with the literature are shown in Table 2. The last row of the table shows the accepted *two-standard-deviation* tolerances proposed by the CSE Working Party [35].

In Table 3 we compared the delineation errors with respect to both the annotators and the inter-cardiologist difference, in the same way proposed in [14].

Finally, we performed a record-by-record classification as proposed in [14] for T-peak and T-end points. For each of the records the average error (*bias*) and standard deviation (*st*) were computed. The records were divided in 4 groups according to the following rules: Group I ($|bias| < 15\ ms$ and $st < 30.6\ ms$), Group II ($|bias| > 15\ ms$ and $st < 30.6\ ms$), Group III ($|bias| < 15\ ms$ and $st > 30.6\ ms$) and Group IV ($|bias| > 15\ ms$ and $st > 30.6\ ms$). For each group the *m* and *s* were computed by averaging the results of each record. The results are shown in Table 4 and Table 5.

3) INTERNAL DATABASE
From the data described in Section II.E for the statistical analysis, 30 seconds from each record were randomly chosen. Two cardiologists annotated the QRS onset, R peaks, T-peaks, T-end points and baseline levels beat by beat. The results of the delineation error of the algorithm when compared to each cardiologist and the inter-cardiologist differences are shown in Table 6.

B. TWA EXTRACTION
We applied the algorithm to the data described in Section II.A.1. Due to the variation of the position of the

TABLE 2. Delineation performance of the proposed algorithm in the QT database. The number of beats analysed, sensitivity (Se), positive predictivity (P+), mean (*m*), standard deviation (*s*) and mean absolute error (|M|) are shown. (N/A: Not Available, N/R: Not Reported).

Method	Parameters	QRS onset	R peak	QRS offset	T-peak	T-end
This work	# Beats	**3623**	**3623**	**3623**	**3542**	**3542**
	Se [%]	**100.00**	**100.00**	**100.00**	**99.50**	**98.73**
	P^+ [%]	**N/A**	**N/A**	**N/A**	**N/A**	**N/A**
	$m \pm s$ [ms]	**2.8 ± 7.7**	**2.2 ± 3.9**	**2.7 ± 9.7**	**-2.6 ± 12.2**	**-2.7 ± 20.7**
	|M| [ms]	**10.1**	**4.9**	**14.0**	**11.6**	**19.0**
Ghaffari et al. [16]	# Beats	N/R	N/R	N/R	N/R	N/R
	Se [%]	99.97	99.97	99.97	99.93	99.93
	P^+ [%]	99.95	99.95	99.95	99.92	99.92
	$m \pm s$ [ms]	-0.6 ± 4.9	0.7 ± 2.4	-0.1 ± 5.9	-0.2 ± 3.1	-0.1 ± 6.8
Ghaffari et al. [15]	# Beats	N/R	N/R	N/R	N/R	N/R
	Se [%]	99.94	99.94	99.94	99.87	99.87
	P^+ [%]	99.91	99.91	99.91	99.80	99.80
	$m \pm s$ [ms]	-0.6 ± 8.0	1.1 ± 2.8	0.3 ± 8.8	0.3 ± 4.1	0.8 ± 10.9
Martinez et al. [14]	# Beats	3623	N/R	3623	3542	3542
	Se [%]	99.97	N/R	99.97	99.77	99.77
	P^+ [%]	N/A	N/R	N/A	97.79	97.79
	$m \pm s$ [ms]	4.6 ± 7.7	N/R	0.8 ± 8.7	0.2 ± 13.9	-1.6 ± 18.1
Martinez et al. [12]	# Beats	3623	N/R	3623	3542	3542
	Se [%]	99.85	N/R	99.85	99.20	99.20
	P^+ [%]	N/R	N/R	N/R	N/R	N/R
	$m \pm s$ [ms]	-0.2 ±7.2	N/R	2.5 ± 8.9	5.3 ± 12.9	5.8 ± 22.7
Tolerances ($2s_{CSE}$) [35]		6.5	-	11.6	-	30.6

TABLE 3. Delineation performance comparison of the presented algorithm and the annotations of two cardiologists. For each fiducial point, the mean (*m*), standard deviation (*s*) and mean absolute error (|M|) are shown.

Validation	QRS on $m \pm s$ [ms] |M| [ms]	R-peak $m \pm s$ [ms] |M| [ms]	QRS off $m \pm s$ [ms] |M| [ms]	T-peak $m \pm s$ [ms] |M| [ms]	T-end $m \pm s$ [ms] |M| [ms]
Algorithm vs *ref1* (all recordings)	2.8 ± 7.7 10.1	2.2 ± 3.9 4.9	2.7 ± 9.7 14.0	-2.6 ± 12.2 11.6	-2.7 ± 20.7 19.0
Algorithm vs *ref1* (11 recordings)	5.9 ± 10.5 11.4	1.8 ± 5 4.8	-1.6 ± 11 12.9	-2.9 ± 10.4 10.8	7.4 ± 18.1 16.9
Algorithm vs *ref2* (11 recordings)	7.9 ± 9.9 12.9	4 ± 3.5 5.1	-2.2 ± 10.2 13.6	-5.8 ± 8.3 7.9	6.6 ± 12.4 12.2
ref1 vs *ref 2* (11 recordings)	5.3 ± 11.1 11.7	-0.6 ± 2.4 1.0	-0.1 ± 12.2 14.2	5.1 ± 15.9 19.8	2.1 ± 22.4 22.0

TABLE 4. QTDB recording stratification according to the performances obtained for T-peak delineation. For each record of the QTDB, the mean error (bias) and standard deviation (std) were used to classify it in: group I (|bias| < 15 ms, std < 30 ms), group II (|bias| > 15 ms, std < 30 ms), group III (|bias| <15 ms, std>30 ms) and group IV (|bias| > 15 ms, std > 30 ms). The percentage of records in each group is shown.

Method	Group I %	Group I $m \pm s$ [ms]	Group II %	Group II $m \pm s$ [ms]	Group III %	Group III $m \pm s$ [ms]	Group IV %	Group IV $m \pm s$ [ms]
This work	**89**	**-5.5 ± 7.7**	**2**	**8.7 ± 22.5**	**3**	**-3.1 ± 55.3**	**6**	**38.1 ± 50.5**
[14]	83	3.9 ± 7.6	5	-2.7 ± 17	5	-0.5 ± 37	7	42 ± 72
[36]	85	-2.7 ± 7.4	2	40 ± 13	1	-7 ±35	12	-48 ± 63
[37]	82	4.2 ±8.6	8	36 ± 15	4	9.6 ± 38	6	32 ± 40

electrodes from subject to subject, we decided to normalize the TWA of each experiment with respect to the mean value obtained during the baseline period. In Fig. 7, the normalized TWA during baseline is compared to the one recorded in supine position after 4 doses of atropine. The statistical analysis revealed that during saline infusion, the normalized

TABLE 5. QTDB recording stratification according to the performances obtained for T-end delineation. For each record of the QTDB, the mean error (bias) and standard deviation (std) were used to classify it in: group I (|bias| < 15 ms, std < 30 ms), group II (|bias| > 15 ms, std<30 ms), group III (|bias| <15 ms, std > 30 ms) and group IV (|bias| > 15 ms, std>30 ms). The percentage of records in each group is shown.

	Group I		Group II		Group III		Group IV	
Method	%	$m \pm s$ [ms]	%	$m \pm s$ [ms]	%	$m \pm s$ [ms]	%	$m \pm s$ [ms]
This work	**77**	**-2.6 ± 13.4**	**5**	**-16.6 ± 25.7**	**8**	**2.2 ± 45.3**	**10**	**-1.5 ± 53.1**
[14]	77	-0.8 ± 12	8	5.8 ± 16	5	-0.6 ± 57	10	-14 ± 46
[36]	63	-2.4 ± 13	9	32 ± 20	6	4 ± 67	22	54 ± 66
[37]	72	7 ± 16	16	31 ± 18	4	9 ± 35	8	49 ± 45

TABLE 6. Delineation performance of the proposed algorithm in the internal database. The number of beats analysed, sensitivity (Se), positive predictivity (P+), mean (*m*), standard deviation (*s*) and mean absolute error (|M|) are shown for each of the two cardiologist (N/A: Not Available). The inter-cardiologist difference is also reported.

| Cardiologist	Parameters	QRS onset	R peak	T-peak	T-end	Baseline [mV]
Cardiologist 1	# Beats	296	294	288	289	294
	Se [%]	100.00	100.00	97.92	97.23	N/A
	P^+ [%]	99.33	98.99	97.58	97.57	N/A
	$m \pm s$ [ms]	15.6 ± 7.2	5.7 ± 4.7	2.2 ± 20.1	-3.3 ± 17.4	-0.0364 ± 0.0021
	$|M|$ [ms]	16.9	8	12.6	17.2	0.0385
Cardiologist 2	# Beats	250	249	238	238	250
	Se [%]	99.60	99.60	95.80	96.20	N/A
	P^+ [%]	99.60	99.60	95.80	95.80	N/A
	$m \pm s$ [ms]	10.9 ± 10.4	2.2 ± 7.5	-1.1 ± 22.2	-9.1 ± 18.9	-0.0416 ± 0.0025
	$|M|$ [ms]	15	6.7	13.9	20.3	0.042
Card1 vs Card 2	$m \pm s$ [ms]	2.9 ± 9	1.5 ± 5.4	1 ± 9.7	6.5 ± 10	0.0036 ± 0.0154
	$|M|$ [ms]	8.6	3.7	7.3	8.9	0.019
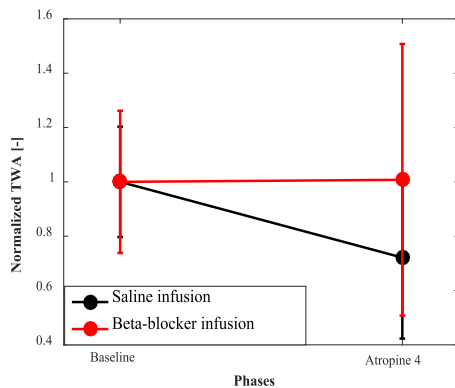
FIGURE 7. Variation of normalized TWA between baseline and supine position after 4 doses of atropine. The results are shown as error bars representing the mean and standard deviation. During saline infusion, the TWA is significantly different from baseline (p-value = 0.005). At the fourth dose of atropine, the TWA during saline infusion is significantly different from beta-blocker infusion (p-value = 0.035).

FIGURE 8. Variation of normalized TWA between baseline and first tilt up. The results are shown as error bars representing the mean and standard deviation. Any significant difference is obtained in this case.

TWA after 4 doses of atropine is significantly different from the baseline level (p-value = 0.005). On the other hand, during beta-blocker infusion, no significant difference is observed. Moreover, we obtained significant difference between normalized TWA in saline and beta-blocker infusion after the 4 doses of atropine (p-value = 0.035).

In Fig. 8, we analysed the variation of normalized TWA between baseline and the first tilt up (without any infusion of atropine). Despite an apparent decrease is observed during
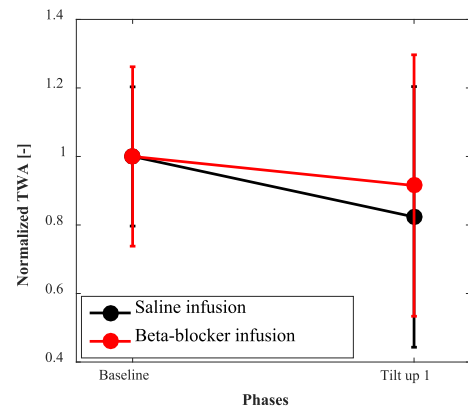
saline infusion, it did not achieved statistical significance (p-value = 0.417). When the saline and beta-blocker infusion in tilted position are compared, a p-value of 0.368 is obtained.

IV. DISCUSSION

The proposed algorithm achieves good results in the delineation of ECG fiducial points.

Concerning the QRS detection, Table 1 shows that in the MITDB our method achieves results that are generally better or comparable with other methods proposed in literature. Other studies, such as the ones of Ghaffari *et al.* [15], [16]

achieve higher performances, but at the same time they used a lower number of true beats, without specifying the ones they did not consider.

As previously specified, our QRS delineator takes inspiration from the work of Merah *et al.* [25] and it can be seen that the performances of the two methods are very similar. Our algorithm introduces the convolution with a Gaussian kernel for the identification of the areas where the QRS complexes are expected. Thanks to this, the set of thresholds based on the RMS of the WT signal proposed in [25] for the identification of significant peaks are not required. This makes the implementation of our QRS detector generally easier than [25].

When our algorithm is validated on the QT database (Table 2), it can be seen that it achieves sensitivity for QRS delineation that is higher than other previously proposed works. Moreover, when the precision in delineation of QRS complexes is considered, our method achieves values of mean m and standard deviation s that are comparable with the other works. This paper uses also the value of the absolute mean error ($|M|$) as a parameter for the evaluation of the performances of the algorithm. Concerning QRS delineation, it can be seen that the algorithm has values of absolute mean error that are lower than 3 samples for QRS onset, approximately one sample for R peak and lower than 4 samples for QRS offset.

Table 2 shows also the sensitivity and delineation accuracy of T-peaks and T-end points. The proposed algorithm achieves good delineation performances for the T-peak, while has some problems in the delineation of T-end (low sensitivity). A deeper analysis showed that the algorithm has problems in detection of the T-end only for sudden death recordings. Further work is needed to improve the algorithm in this type of condition. Moreover, our method combines two previously proposed algorithms for T-end delineation and the results show that this does not significantly improve the overall performance and that the original ACL method proposed in [15] has higher sensitivity than the combination proposed in this study. The combination of the two methods was necessary for correcting wrongly detected biphasic T-waves as shown in Fig. 4(c) and 5(d). This correction was particularly necessary in the data of the experimental database for which TWA was calculated and we could not avoid it by implementing only the method proposed in [15]. In other words, we preferred gaining precision in T-peak delineation than in T-end location because of the purpose of having a good estimate of TWA.

Concerning the delineation accuracy in the QTDB, our algorithm has values of m and s that are comparable with [12] and [14], while they are worse than [15] and [16]. It should be noted that in [15] and [16] the authors did not just use the annotations, but they asked two cardiologists to re-annotate the ECG and they then used the re-annotated signals for the validation. This fact may be misleading in the results obtained. Nevertheless, our algorithm is able of delineating T-peaks and T-ends with an absolute mean error less than 3 samples and less than 5 samples respectively.

The last row of Table 2 shows the tolerances of the standard deviation of the delineation error proposed in [35]. Our algorithm has values of s that are lower than the tolerance for QRS offsets and T-ends, while the goal is nearly achieved for QRS onset.

Table 3 shows that the error in delineation accuracy of our algorithm with both the cardiologists is lower or comparable with the inter-cardiologist difference. This means that the developed algorithm has performances that are comparable to the human error.

The stratification of the recordings of the QT database shown in Table 4 and V show that the proposed algorithm is able of detecting precisely the T-peak in the 89% of the recordings, thus outperforming other previous works. The performances for the T-end point are comparable to the ones achieved in [14].

Therefore, the validation in the QT database shows that our algorithm has performances that are comparable with or higher than other state of the art algorithms and comparable with the human error. When other WT-based algorithm are considered (e.g. [13]–[16]) it can be seen that our algorithm is able of delineating the ECG fiducial points by using only one scale of the WT and does not require information from more scales. Thus, our algorithm requires less information to be stored than [13]–[16]. In addition, the implementation of our algorithm is easier than previously published works since it does not require the large amount of adaptive thresholds proposed in in [13]–[16]. The algorithm is based only on the calculation of the indexes s and S for the detection of R-peaks and T-peaks. Concerning computational complexity, our algorithm uses two different wavelet filters for QRS complexes and T-waves, thus increases the computational cost if compared to methods using only one filter. However, with state-of-the-art computational power this cannot be considered a limitation of our method.

In Table 6 the results of the validation of the algorithm in the internal database are shown. Despite the low number of annotations, the results were considered acceptable by clinical staff. In particular, the T-peak and the baseline level are annotated with precision that is comparable to the inter-cardiologist difference. The high value of standard deviation for the T-peak is due to a record where few mistakes in T-peak delineation were present due to a large amount of noise in the data set. It should be noticed that for R-peaks the delineation accuracy of the algorithm is higher than the inter-cardiologist difference. This is due to the fact that in one record the algorithm recognized S-waves as R-peaks due to their abnormally high absolute value.

The results obtained with the validations suggest that our algorithm has good precision in the identification of ECG fiducial points.

The algorithm was designed for 1kHz sampling frequency and for validation in the MIT/BIH and QTDB it was applied with different wavelet scales and parameter λ in order to

select the regions of QRS and T-waves due to the different sampling frequencies and not to alter the manual annotations. In order not to let the users select the appropriate scale, it is suggested that in future applications the signals are resampled at 1 kHz and then the algorithm applied. This was tried with other clinical signals and it was visually checked by clinicians that the algorithm is still performing well.

This automatic method was then applied to data recorded with different activation and/or blockage of the PNS and SNS. Fig. 7 shows that atropine alone decreases significantly TWA when compared to baseline level. When the subjects are given beta-blocker, such decrease is not observed and TWA remains at the same level of the baseline level. These results confirm the observations obtained in previous studies [8], [9]. In particular, the blockage of the PNS causes a decrease of TWA and beta-blocker drugs cause an increase.

In Fig. 8, the effects of the activation of SNS are shown. However, we did not find any significant difference in TWA due to the activation of the SNS. It can be stated that the increasing of sympathetic activity decreases TWA, but not significantly.

Because of the physiological origin of the T-wave, these results show that the automatic measurement of TWA can give information on the status of the innervation of the myocardium. In particular, a decrease in TWA can be related to an activation of the SNS or the blockage of the PNS, while an increase in TWA can be interpreted as a blockage of the SNS.

V. CONCLUSIONS

We have presented a new robust wavelet-based algorithm for the automatic delineation of QRS onsets, R peaks, QRS offsets, T-wave peaks, T-end points and estimation of the baseline level in the TP segment in one-lead ECG signals. The algorithm is able of delineating three different T-wave morphologies: upwards, inverted and biphasic T-waves.

The algorithm has been validated with different databases and the results obtained show that it achieves performances that are generally comparable with or higher than other previous algorithms. Moreover, the delineation accuracy of the algorithm is comparable with the inter-cardiologist delineation difference.

For the first time, an automatic method was applied for the evaluation of T-wave amplitude (TWA) and its interpretation as marker of the innervation of the myocardium. In particular, it was observed that blockage of the PNS causes a significant decrease of TWA, while blockage of the SNS causes its increase. These already known results confirm the reliability of the presented algorithm.

The achieved results support the idea that this automatic method may be used as a useful tool in clinical practice for the calculation of TWA and the evaluation of the autonomic innervation of the myocardium.

REFERENCES

[1] R. C. Drew and L. I. Sinoway, "Autonomic control of the heart," in *Primer on the Autonomic Nervous System*. Amsterdam, The Netherlands: Academic, 2012, pp. 177–180.

[2] J. Sztajzel, "Heart rate variability: A noninvasive electrocardiographic method to measure the autonomic nervous system," *Swiss Med. Weekly*, vol. 134, nos. 35–36, pp. 514–522, 2004.

[3] Task Force of The European Society of Cardiology and The North American Society of Pacing and Electrophysiology, "Heart rate variability," *Eur. Heart J.*, vol. 17, pp. 354–381, 1996.

[4] H. M. Stauss, "Heart rate variability," *Amer. J. Physiol.-Regulatory, Integr. Comparative Physiol.*, vol. 285, no. 5, pp. 927–931, 2003.

[5] M. J. Shen and D. P. Zipes, "Role of the autonomic nervous system in modulating cardiac arrhythmias," *Circulat. Res.*, vol. 114, no. 6, pp. 1004–1021, Mar. 2014.

[6] M. R. Franz, K. Bargheer, A. Costard-Jäckle, D. C. Miller, and P. R. Lichtlen, "Human ventricular repolarization and T wave genesis," *Prog. Cardiovascular Diseases*, vol. 33, no. 6, pp. 369–384, 1991.

[7] G.-X. Yan and C. Antzelevitch, "Cellular basis for the normal T wave and the electrocardiographic manifestations of the long-QT syndrome," *Circulation*, vol. 98, pp. 1928–1936, Nov. 1998.

[8] R. J. Contrada *et al.*, "Effects of beta-adrenergic activity on t-wave amplitude," *Psychophysiology*, vol. 26, no. 4, pp. 488–492, 1989.

[9] S. Fukudo *et al.*, "Accentuated vagal antagonism of beta-adrenergic effects on ventricular repolarization. Evidence of weaker antagonism in hostile type A men," *Circulation*, vol. 85, no. 6, pp. 2045–2053, 1992.

[10] M. Baumert *et al.*, "Cardiac repolarization variability in patients with postural tachycardia syndrome during graded head-up tilt," *Clin. Neurophysiol.*, vol. 122, no. 2, pp. 405–409, Feb. 2011.

[11] R. van Lien, M. Neijts, G. Willemsen, and E. J. C. de Geus, "Ambulatory measurement of the ECG T-wave amplitude," *Psychophysiology*, vol. 52, no. 2, pp. 225–237, 2015.

[12] A. Martínez, R. Alcaraz, and J. J. Rieta, "A new method for automatic delineation of ECG fiducial points based on the Phasor transform," in *Proc. Annu. Int. Conf. IEEE Eng. Med. Biol. (EMBC)*, vol. 10. Aug. 2010, pp. 4586–4589.

[13] C. Li, C. Zheng, and C. Tai, "Detection of ECG characteristic points using wavelet transforms," *IEEE Trans. Biomed. Eng.*, vol. 42, no. 1, pp. 21–28, Jan. 1995.

[14] J. P. Martinez, R. Almeida, S. Olmos, A. P. Rocha, and P. Laguna, "A wavelet-based ECG delineator: Evaluation on standard databases," *IEEE Trans. Biomed. Eng.*, vol. 51, no. 4, pp. 570–581, Apr. 2004.

[15] A. Ghaffari, M. R. Homaeinezhad, M. Akraminia, M. Atarod, and M. Daevaeiha, "A robust wavelet-based multi-lead electrocardiogram delineation algorithm," *Med. Eng. Phys.*, vol. 31, no. 10, pp. 1219–1227, Dec. 2009.

[16] A. Ghaffari, M. R. Homaeinezhad, M. Khazraee, and M. M. Daevaeiha, "Segmentation of holter ECG waves via analysis of a discrete wavelet-derived multiple skewness-kurtosis based metric," *Ann. Biomed. Eng.*, vol. 38, no. 4, pp. 1497–1510, 2010.

[17] G. de Lannoy, B. Frenay, M. Verleysen, and J. Delbeke, "Supervised ECG delineation using the wavelet transform and hidden Markov models," in *Proc. 4th Eur. Conf. Int. Fed. Med. Biol. Eng.*, 2009, pp. 22–25.

[18] R. V. Andreão and J. Boudy, "Combining wavelet transform and hidden Markov models for ECG segmentation," *EURASIP J. Adv. Signal Process.*, vol. 2007, Dec. 2007, Art. no. 056215.

[19] O. Sayadi and M. B. Shamsollahi, "A model-based Bayesian framework for ECG beat segmentation," *Physiol. Meas.*, vol. 30, no. 3, pp. 335–352, 2009.

[20] M. Cesari, J. Mehlsen, A. B. Mehlsen, and H. B. D. Sorensen, "Application of a new robust ECG T-wave delineation algorithm for the evaluation of the autonomic innervation of the myocardium," in *Proc. 38th Annu. Int. Conf. IEEE Eng. Med. Biol. Soc. (EMBC)*, Aug. 2016, pp. 3801–3804.

[21] G. B. Moody and R. G. Mark, "The impact of the MIT-BIH arrhythmia database," *IEEE Eng. Med. Biol. Mag.*, vol. 20, no. 3, pp. 45–50, May/Jun. 2001.

[22] P. Laguna, R. G. Mark, A. Goldberg, and G. B. Moody, "A database for evaluation of algorithms for measurement of QT and other waveform intervals in the ECG," in *Proc. Comput. Cardiol.*, vol. 24. Sep. 1997, pp. 673–676.

[23] K. Najarian and R. Splinter, *Biomedical Signal and Image Processing*. Boca Raton, FL, USA: CRC Press, 2012.

[24] S. Mallat, "Zero-crossings of a wavelet transform," *IEEE Trans. Inf. Theory*, vol. 37, no. 4, pp. 1019–1033, Jul. 1991.

[25] M. Merah, T. A. Abdelmalik, and B. H. Larbi, "R-peaks detection based on stationary wavelet transform," *Comput. Methods Programs Biomed.*, vol. 121, no. 3, pp. 149–160, Oct. 2015.

[26] O. Guven, A. Eftekhar, R. Hoshyar, G. Frattini, W. Kindt, and T. G. Constandinou, "Realtime ECG baseline removal: An isoelectric point estimation approach," in *Proc. IEEE Biomed. Circuits Syst. Conf. (Bio-CAS)*, Oct. 2014, pp. 29–32.

[27] L. Burattini and C. Giuliani, "T-wave frequency content evaluation in healthy subjects and patients affected by miocardial infarction," in *Signal Processing New Research*. Hauppauge, NY, USA: Nova, 2013, pp. 79–93.

[28] K. Sembulingam, and P. Sembulingam, *Essentials of Medical Physiology*. London, U.K.: JP Medical, 2012, pp. 551–558.

[29] Q. Zhang, A. I. Manriquez, C. Medigue, Y. Papelier, and M. Sorine, "An algorithm for robust and efficient location of T-wave ends in electrocardiograms," *IEEE Trans. Biomed. Eng.*, vol. 53, no. 12, pp. 2544–2552, Dec. 2006.

[30] R. Almeida, J. P. Martínez, S. Olmos, A. P. Rocha, and P. Laguna, "Automatic delineation of T and P waves using a wavelet-based multiscale approach," in *Proc. 1st Int. Congr. Comput. Bioeng.*, 2003, pp. 243–247.

[31] S. Banerjee, R. Gupta, and M. Mitra, "Delineation of ECG characteristic features using multiresolution wavelet analysis method," *Measurement*, vol. 45, no. 3, pp. 474–487, Apr. 2012.

[32] D. Benitez, P. A. Gaydecki, A. Zaidi, and A. P. Fitzpatrick, "The use of the Hilbert transform in ECG signal analysis," *Comput. Biol. Med.*, vol. 31, no. 5, pp. 399–406, Sep. 2001.

[33] D. B. Saadi *et al.*, "Automatic real-time embedded QRS complex detection for a novel patch-type electrocardiogram recorder," *IEEE J. Transl. Eng. Health Med.*, vol. 3, Nov. 2015, Art. no. 1900112.

[34] J. Pan and W. J. Tompkins, "A real-time QRS detection algorithm," *IEEE Trans. Biomed. Eng.*, vol. BME-32, no. 3, pp. 230–236, Mar. 1985.

[35] J. L. Willelms, "Recommendations for measurement standards in quantitative electrocardiography. The CSE working party," *Eur. Heart J.*, vol. 6, no. 10, pp. 815–825, 1985.

[36] R. Jane, A. Blasi, J. Garcia, and P. Laguna, "Evaluation of an automatic threshold based detector of waveform limits in Holter ECG with the QT database," in *Proc. Comput. Cardiol.*, vol. 24. Sep. 1997, pp. 295–298.

[37] J. A. Vila, Y. Gang, J. M. R. Presedo, M. Fernández-Delgado, S. Barro, and M. Malik, "A new approach for TU complex characterization," *IEEE Trans. Biomed. Eng.*, vol. 47, no. 6, pp. 764–772, Jun. 2000.

[38] P. B. Brockhoff. (2015). *Repeated Measurements, Part 1, Simple Methods*. [Online]. Available: http://02429.compute.dtu.dk/enote/afsnit/NUID191/

[39] P. B. Brockhoff. (2015). *Repeated Measures, Part 2, Advanced Methods*. [Online]. Available: http://02429.compute.dtu.dk/enote/afsnit/NUID192/

JESPER MEHLSEN received the Medical degree from the University of Copenhagen in 1979. He became a Specialist in clinical physiology and nuclear medicine in 1990. Since 2010, he has been the Head of Research with the Coordinating Research Center, Bispebjerg and Frederiksberg Hospitals, where he has also been the Chief Physician with the Syncope Center, Cardiology Department, since 2016.

ANNE-BIRGITTE MEHLSEN received the Medical degree from the University of Odense in 1995. She became a Specialist in clinical physiology and nuclear medicine in 2007. Since 2015, she has been a Senior Consultant with the Department of Clinical Physiology, Nuclear Medicine and Pet, Rigshospitalet, Copenhagen.

MATTEO CESARI (M'16) received the bachelor's degree (Hons.) in information engineering from the University of Padova, Italy, in 2013, the master's degrees in biomedical engineering from the University of Padova and the Technical University of Denmark, in the context of the Top Industrial Manager for Europe (T.I.M.E.) double degree program. He is currently pursuing the Ph.D. degree with the Department of Electrical Engineering, Technical University of Denmark. His research interests include automatic biomedical signal processing, algorithm design, and clinical validations.

HELGE BJARUP DISSING SORENSEN (M'90) received the M.S.E.E. and Ph.D. degrees in electrical engineering from the Institute of Electronic Systems, Alborg University, in 1985 and 1992, respectively. He was initially a Research Assistant with Aalborg University. From 1989 to 1993, he was an Assistant Professor with the Institute of Electronic Engineering, Alborg University. From 1993 to 1995, he was an Associate Professor with the Engineering Academy Denmark. Since 1995, he has been an Associate Professor and since 2007, the Leader of the Biomedical Signal Processing Research Group, Biomedical Engineering, Department of Electrical Engineering, Technical University of Denmark.